Supplementary information
A continuum model for lithium plating and dendrite formation in lithium-ion batteries: formulation and validation against experiment

Smita Sahu[1,2,3] and Jamie M. Foster[1,2,4]

[1]School of Mathematics and Physics, University of Portsmouth, Lion Terrace, PO1 3HF, UK
[2]The Faraday Institution, Quad One, Becquerel Avenue, Harwell Campus, Didcot, OX11 0RA, UK
[3]smita.sahu@port.ac.uk
[4]jamie.michael.foster@gmail.com

December 1, 2022

1 Numerical solution of SPM with plating model

We use second-order finite element approximation given in[1] for radial discretisation in r of the microscopic equations and MATLAB's `ode15s` routine for time integration. We introduce a set of points r_i, $i = 0, \ldots, N$ with step size $\Delta_r = r_{i+1} - r_i$ and denote the corresponding values of $c_a^i(t), \psi_a(t), C_{\text{tot}}(t), C_{\text{in}}(t), c_c^i(t), \psi_c(t)$, for galvanostatic (dis)charge where the current was considered as an input and voltage as an output. For potentiostatic (dis)charge (where the voltage was considered as an input and current as an output) corresponding values are $c_a^i(t), \psi_a^i(t), C_{\text{tot}}(t), C_{\text{in}}(t), c_c^i(t), \psi_c^i(t), I^i(t))$. In total, we have $2N + 4$ equations and our solution vector thus consists of a total of $2N + 4$ unknowns. We assemble the unknown functions of time into one large vector $\mathbf{u}(t)$ as follows

$$\mathbf{u}(t) = [c_a^1, ..., c_a^2, ..., c_a^N, \psi_a, C_{\text{tot}}, C_{\text{in}}, c_c^1, ..., c_c^2, ..., c_c^N, \psi_c]' \tag{1}$$
$$= [\mathbf{c_a}(t), \psi_a(t), C_{\text{tot}}(t), C_{\text{in}}(t), \psi_c(t), \mathbf{c_c}(t)]' \tag{2}$$

This leads us to the following system of DAEs

$$\mathbf{M}\frac{d\mathbf{u}}{dt} = \mathbf{f}(\mathbf{u}), \qquad \text{with} \qquad \mathbf{u}|_{t=0} = \mathbf{u}_0. \tag{3}$$

Here $\mathbf{M}_{(2N+4)\times(2N+4)}$ is the mass matrix whose entries are coefficients of the time derivatives and the function $\mathbf{f}(\mathbf{u})$ is non-linear and returns a vector of dimension $2N + 4$. Its entries

represent the right-hand side of the discretised equations. To solve this temporal system of DAEs we use `ode15s` from MATLAB. Note that for potentiostatic (discharge) our solution vector will be $\mathbf{u} = [\mathbf{c_a}(t), \psi_a(t), C_{\text{tot}}(t), C_{\text{in}}(t), \psi_c(t), \mathbf{c_c}(t), I(t)]^T$ and the size of the mass matrix will also increase by one row and column *i.e.* $(2N+5) \times (2N+5)$.

1.1 Conservation properties

In this section, we will derive the conservation properties of Li in each phase. These have been used as a validation that the numerical method performs as expected.

Total Li concentration in mols in anode particles The total concentration of Li in the anode particles is denoted by C_a and give by

$$C_a = \iiint_{\Omega_a} c_a dV_{\Omega_a}$$

where c_a is the Li-ion concentration in anode particles and $\Omega_a = (0, R_a)$ is the region where we compute the total concentration of Li in anode particles. By equation (2) from the main paper

$$\iiint_{\Omega_a} \frac{\partial c_a}{dt} dV_{\Omega_a} = \iiint_{\Omega_a} \frac{1}{r_a^2} \frac{\partial}{\partial r_a} \left(r_a^2 D_a(c_a, T) \frac{\partial c_a}{\partial x} \right) dV_{\Omega_a}$$

By the divergence theorem we get

$$\tfrac{dC_a}{dt} = -\iint_{\partial\Omega_a} (\mathcal{F}_{c_a} \cdot \hat{\mathbf{n}}_{\mathbf{c_a}})\, dS,$$

here $\partial\Omega_a$ is the boundary of region Ω_a and $\hat{\mathbf{n}}_{\mathbf{c_a}}$ is unit normal vector to the surface $\partial\Omega_a$. Hence the rate of change in the total concentration of Li in graphite particles is given below

$$\frac{dC_a}{dt} = -4\pi R_a^2 \left(\xi_e \frac{j_{\text{ae}}}{F} - \xi_p m_{\text{pa}} \right). \tag{4}$$

and

$$C_a \;\; = \iiint_{\Omega_a} c_a dV_{\Omega_a} = \int_0^{R_a} \int_0^{2\pi} \int_0^{\pi} c_a r^2 \sin(\phi) d\phi d\theta dr = 4\pi \int_0^{R_a} r^2 c_a dr. \tag{5}$$

Total Li concentration in mols in cathode particles The total concentration of Li in the cathode particles is denoted by C_c and given by

$$C_c = \iiint_{\Omega_c} c_c dV_{\Omega_c}$$

where c_c is the Li-ion concentration in the cathode and $\Omega_c = (0, R_c)$ is the region where we compute the total concentration of Li in cathode particles. By equation (24) from the main paper

$$\iiint_{\Omega_c} \tfrac{\partial c_c}{dt} dV_{\Omega_c} = \iiint_{\Omega_c} \tfrac{1}{r_c^2} \tfrac{\partial}{\partial r_c} \left(r_c^2 D_c(c_c) \tfrac{\partial c_c}{\partial x} \right) dV_{\Omega_c}$$

By the divergence theorem, we get

$$\frac{dC_c}{dt} = -\iint_{\partial\Omega_c} (\mathcal{F}_{c_c} \cdot \hat{\mathbf{n}}_{\mathbf{c_c}})\, dS,$$

here $\partial\Omega_c$ is the boundary of region Ω_c and $\hat{\mathbf{n}}_{\mathbf{c_c}}$ is unit normal vector to the surface $\partial\Omega_c$. Hence the rate of change in total concentration of Li in cathode particles is given below

$$\frac{dC_c}{dt} = -4\pi R_c^2 \frac{j_{\text{ce}}}{F} \tag{6}$$

where

$$C_c \;= \iiint_{\Omega_c} c_c dV_{\Omega_c} = \int_0^{R_c}\int_0^{2\pi}\int_0^{\pi} c_c r^2 \sin(\phi) d\phi d\theta dr = 4\pi \int_0^{R_c} r^2 \tfrac{\partial c_c}{\partial t} dr. \tag{7}$$

Now we can claim that Li is conserved throughout the system.

2 The DFN model with Li plating

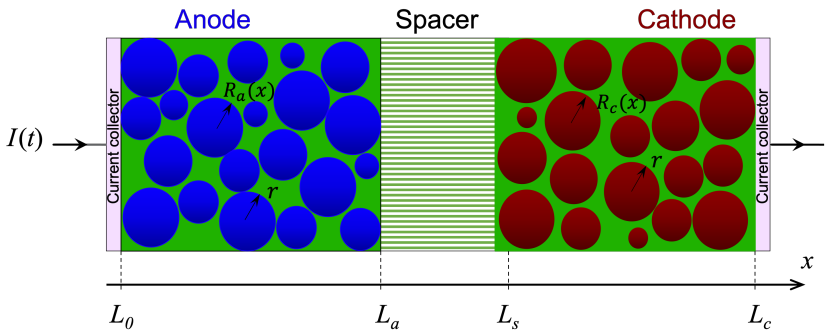

Figure 1: A schematic of the full cell geometry.

In this section, we extend our SPM with Li plating model to DFN with Li plating model. For notation purposes, we follow the equations given in [1]. We consider the DFN model posed on a one-dimensional cell lying between $x = L_0$, $x = L_c$ (as illustrated Fig. 1) consisting of an anode in $L_0 < x < L_a$, a separator in $L_a < x < L_s$, and a cathode in $L_s < x < L_c$. As shown in Fig. 2 in the main paper, the thin layer on the surface of the graphite particle is comprised of several phases, namely plated Li, electrolyte, and SEI. Therefore

$$\xi_s + \xi_p(x,t) + \xi_e(x,t) = 1 \tag{8}$$

pertains in the surface layer, where ξ_s is the constant volume fraction of SEI, ξ_p is the volume fraction of plated Li and ξ_e is the volume fraction of electrolyte. The equation governing ionic transport through the electrolyte

$$\frac{\partial(\epsilon_l c)}{\partial t} + \frac{\partial N_-}{\partial x} = 0, \quad N_- = -\mathcal{B}(\epsilon_l) D_{\text{e}}(c) \frac{\partial c}{\partial x} - (1 - t_0^+)\frac{j}{F} \quad \text{in} \quad L_0 < x < L_c, \tag{9}$$

where x is the position through the electrode and t is the time and the volume fraction of electrolyte (porosity) is defined as

$$\epsilon_l(x, C_{\text{out}}, t) = \begin{cases} 1 - \epsilon_a - \epsilon_d(x,t) & \text{in} \quad L_0 \leq x < L_a, \\ \epsilon_s & \text{in} \quad L_a < x < L_s, \\ 1 - \epsilon_c & \text{in} \quad L_s \leq x < L_c, \end{cases} \tag{10}$$

and initial porosity is

$$\epsilon_l|_{t=0} = \begin{cases} 1 - \epsilon_a & \text{in} \quad L_0 \leq x < L_a, \\ \epsilon_s & \text{in} \quad L_a < x < L_s, \\ 1 - \epsilon_c & \text{in} \quad L_s \leq x < L_c, \end{cases} \tag{11}$$

where ϵ_a is the volume fraction of anode particles in the anode, ϵ_s is the local volume fraction of electrolyte in separator, and ϵ_c is the volume fraction of cathode particles, ϵ_d is the volume fraction of plated Li and given as

$$\epsilon_d = n_a \frac{C_{\text{out}} V_{\text{Li}}}{A L_a} \tag{12}$$

where n_a is the total number of particles in the anode which is given by $n_a = AL_a\epsilon_a/(4\pi R_a^3/3)$ where A is the cross-section area of the cell and L_a is the thickness of the anode. C_{out} is the concentration of irreversible plated Li in mols, V_{Li} is the partial molar volume of Li-metal, c is the molar concentration of ions in the electrolyte, N_- is the effective flux of anions across the electrolyte, D is the ionic diffusivity of the electrolyte and $\mathcal{B}$ is the permeability factor is given by Bruggeman relation

$$\mathcal{B}(\epsilon_l) = \epsilon_l^{1.5}(x, C_{\text{out}}, t) \tag{13}$$

t^+ is the transference number, j is the ionic current density and F is Faraday's constant. In contrast to some other authors, we opt to write the conservation equation in terms of the anion flux, N_-. The ionic current in the electrolyte given by

$$\frac{\partial j}{\partial x} = \begin{cases} b_{ae} j_{\text{ae}} + b_{pe} j_{\text{pe}} & \text{in} \quad L_0 \leq x < L_a, \\ 0 & \text{in} \quad L_a < x < L_s, \\ b_{ce} j_{\text{ce}} & \text{in} \quad L_s \leq x < L_c, \end{cases} \tag{14}$$

$$j = -\mathcal{B}(\epsilon_l)\kappa(c)\left(\frac{\partial \Phi}{\partial x} - \frac{2RT}{F}\frac{1 - t_0^+}{c}\frac{\partial c}{\partial x}\right) \quad \text{in} \quad L_0 < x < L_c, \tag{15}$$

here $b_{ae} = 4\pi R_a^2 n_a \xi_e / AL_a$ is the surface area between anode particles and electrolyte per unit volume of the anode, $b_{pe} = n_a \left(A_{\text{pe}}\xi_p + \mathcal{N}\right)/AL_a$ is the surface area between plate and electrolyte per volume of anode (with units of m^{-1}), A_{pe} is the total surface of the pores in the SEI and $\mathcal{N}$ is the area of the graphite's surface where nucleation can occur given in Fig. 2 of the main paper. j_{ae} is the reaction rate which is zero in the separator and given by the Butler-Volmer equations in the electrode and it is zero in the separator given in (38), j_{pe} is the current density due to the oxidisation of Li metal directly into the electrolyte given in (42), b_{ce} is the surface area between cathode particles and electrolyte per unit volume of cathode

and $j_{\rm ce}$ is the reaction rate from cathode to electrolyte given in equation (40). κ is the ionic conductivity, Φ is the electric potential in the electrolyte, R is the (molar/universal/ideal) gas constant and T is the absolute temperature. The electric transport through the anode is given by

$$\frac{\partial j_a}{\partial x} = -\left(b_{ae} j_{\rm ae} + b_{pe} j_{\rm pe}\right), \quad \text{in} \quad L_0 < x < L_a, \tag{16}$$

$$j_a = -\sigma_a \frac{\partial \Phi_a}{\partial x}, \quad \text{in} \quad L_0 < x < L_a, \tag{17}$$

$$b_{pe} j_{\rm pe} = \frac{1}{AL_a}\left(A_{\rm pe}\xi_p j_{\rm pe} + \mathcal{N}\left(j_{\rm pe}^{+}\mathcal{H}(\xi_p) + j_{\rm pe}^{-}\right)\right). \tag{18}$$

The electric transport through the cathode is given by

$$\frac{\partial j_c}{\partial x} = -b_{ce} j_{\rm ce}, \quad j_c = -\sigma_c \frac{\partial \Phi_c}{\partial x}, \quad \text{in} \quad L_s < x < L_c, \tag{19}$$

where the macroscopic boundary and initial conditions on the model are

$$j_a|_{x=L_0} = \frac{I(t)}{A}, \quad N_-|_{x=L_0} = 0, \quad j|_{x=L_0} = 0, \quad j_a|_{x=L_a} = 0, \tag{20}$$

$$j_c|_{x=L_s} = 0, \qquad j_c|_{x=L_c} = \frac{I(t)}{A}, \quad N_-|_{x=L_c} = 0, \quad j|_{x=L_c} = 0, \tag{21}$$

representing galvanostatic discharge at a current $I(t)$ which flows into the anode current collector on $x = L_0$ through the anode particles and out through the cathode current collector on $x = L_c$ through the cathode particles (Fig. 1). No electronic current passes through the electronically insulating separator. Li transport equations posed in representative spherical electrode particles which occupy the regions $0 \le r \le R_a(x)$ in the anode $L_0 < x < L_a$ and $0 \le r \le R_c(x)$ in the cathode ($L_s < x < L_c$), where $R_a(x)$ and $R_c(x)$ are allowed to vary in space. The microscopic equations and boundary conditions on the anode are given by

$$\left.\begin{array}{l} \dfrac{\partial c_a}{\partial t} = \dfrac{1}{r^2}\dfrac{\partial}{\partial r}\left(r^2 D_a(c_a,T)\dfrac{\partial c_a}{\partial r}\right) \quad \text{in} \quad 0 < r < R_a(x) \\ -D_a(c_a,T)\dfrac{\partial c_a}{\partial r}\Big|_{r=R_a(x)} = 0, \quad -D_a(c_a,T)\dfrac{\partial c_a}{\partial r}\Big|_{r=R_a(x)} = \xi_e j_{\rm ae}/F - \xi_p m_{\rm pa} \end{array}\right\} \text{ in } L_0 < x < L_a, \tag{22}$$

and on cathode given by

$$\left.\begin{array}{l} \dfrac{\partial c_c}{\partial t} = \dfrac{1}{r^2}\dfrac{\partial}{\partial r}\left(r^2 D_c(c_c,T)\dfrac{\partial c_c}{\partial r}\right) \quad \text{in} \quad 0 < r < R_c(x) \\ D_c(c_c,T)\dfrac{\partial c_c}{\partial r}\Big|_{r=R_c(x)} = 0, \quad -D_c(c_c,T)\dfrac{\partial c_c}{\partial r}\Big|_{r=R_c(x)} = j_{\rm ce}/F \end{array}\right\} \text{ in } L_s < x < L_c, \tag{23}$$

The total number of mols of Li plated on the surface of the anode particle (in both reversible and irreversible form), $C_{\rm tot}$, is given by

$$\frac{dC_{\rm tot}}{dt} = -4\pi R_a^2 m_{\rm pa}\xi_p - \frac{j_{\rm pe}}{F}A_{\rm pe}\xi_p - \frac{\mathcal{N}}{F}\left(j_{\rm pe}^{+}\mathcal{H}(\xi_p) + j_{\rm pe}^{-}\right), \tag{24}$$

$$C_{\rm tot}|_{t=0} = 0, \tag{25}$$

recoverable plated Li is account by

$$\frac{dC_{\text{in}}}{dt} = \begin{cases} \dfrac{dC_{\text{tot}}}{dt} & \text{if} \quad 0 < \xi_p < \xi_p^{\bullet} \quad \text{or} \quad \frac{dC_{\text{tot}}}{dt} \leq 0 \\ 0 & \text{otherwise} \end{cases}, \tag{26}$$

and dead plated Li is account by

$$\frac{dC_{\text{out}}}{dt} = \begin{cases} 0 & \text{if} \quad 0 < \quad \xi_p < \xi_p^{\bullet} \quad \text{or} \; \frac{dC_{\text{tot}}}{dt} \leq 0 \\ \dfrac{dC_{\text{tot}}}{dt} & \text{otherwise} \end{cases}, \tag{27}$$

where $\xi_p^{\bullet} \leq 1 - \xi_s$ is the threshold volume fraction of the surface film that the Li metal can occupy before it starts to grow outside with SEI (illustrated in Fig. 2 of the main paper), where $s_a - R_a$ is the SEI thickness. We equip the following initial conditions

$$C_{\text{in}}|_{t=0} = 0, \quad C_{\text{out}}|_{t=0} = 0. \tag{28}$$

Summing (26) and (27), integrating with respect to time and imposing (25) and (28) leads to the reassuring conclusion that

$$C_{\text{tot}} = C_{\text{in}} + C_{\text{out}}. \tag{29}$$

The volume fraction of the surface film occupied by Li metal and the number of mols of recoverable Li metal are related via

$$C_{\text{in}} = \frac{4\pi\xi_p(s_a^3 - R_a^3)}{3V_{Li}}, \tag{30}$$

Initial conditions are provided for the ion concentration in the electrolyte

$$c|_{t=0} = c_0, \tag{31}$$

and likewise for those in the active materials in the anode and cathode are given by

$$c_a|_{t=0} = c_{a,0}, \quad c_c|_{t=0} = c_{c,0}, \tag{32}$$

When considering battery safety it is of paramount importance to be able to discern when dendrites are inert and when they are live and a potential source of short-circuiting. Li metal outside of the porous SEI is apportioned into two phases; C_{out}^{+} denotes Li metal outside the SEI that remains electronically connected to the anode whilst C_{out}^{0} denotes Li metal outside the SEI that is electronically disconnected and therefore inert/dead. We have

$$C_{\text{out}} = C_{\text{out}}^{+} + C_{\text{out}}^{0}. \tag{33}$$

We assume that as Li metal grows outside of the SEI it does so in the form of dangerous live dendrites. These electronically connected dendrites become severed from the anode if, at a later time, all of the Li metal within the porous SEI has been oxidised such that there

is no longer an electronically conducting material bridging the SEI film and connecting the dendrites to the graphite. Hence

$$\begin{cases} C^{+}_{\text{out}} = 0 & \text{when} \quad \xi_p = 0, \\ \dfrac{dC^{+}_{\text{out}}}{dt} = \dfrac{dC_{\text{out}}}{dt} & \text{otherwise.} \end{cases} \tag{34}$$

Notably, these equations have the properties that

$$j + j_a = \frac{I(t)}{A} \quad \text{in} \quad L_0 < x < L_a, \tag{35}$$

$$j + j_c = -\frac{I(t)}{A} \quad \text{in} \quad L_s < x < L_c, \tag{36}$$

$$\int_{L_1}^{L_2} \left(b(x) j_n + b_{pe} n_a \frac{C_{\text{tot}}}{A L_a} \right) dx = \frac{I}{A}, \tag{37}$$

The (de)intercalation reaction in the anode is given by the following Butler-Volmer (BV) equation

$$j_{\text{ae}} = 2F k_{\text{ae}} \sqrt{c_e c_a|_{r_a=R_a} \left(c_a^{\max} - c_a|_{r_a=R_a}\right)} \sinh\left(\frac{F\eta_{ae}}{2RT}\right), \tag{38}$$

$$\eta_{ae} = \Phi_a - \Phi - U_{eq,a}(c_a|_{r=R_a(x)}) \tag{39}$$

here k_{ae} is the reaction rate constant. The (de)intercalation reaction in cathode is given by the following BV equation

$$j_{\text{ce}} = 2F k_{\text{ce}} \sqrt{c_e c_c|_{r_c=R_c} \left(c_a^{\max} - c_c|_{r_c=R_c}\right)} \sinh\left(\frac{F\eta_{ce}}{2RT}\right), \tag{40}$$

$$\eta_{ce} = \Phi_c - \Phi - U_{eq,c}(c_c|_{r=R_c(x)}), \tag{41}$$

k_{ce} is a reaction rate constant. The current density due to the oxidisation of Li metal directly into the electrolyte, j_{pe}, is given by

$$j_{\text{pe}} = 2F k_{\text{pe}} \sqrt{\frac{c_e}{V_{Li}}} \sinh\left(\frac{F\eta_{pe}}{2RT}\right), \tag{42}$$

where η_{pe} is the overpotential between Li plating and electrolyte and given by

$$\eta_{pe} = \Phi_a - \Phi - \Delta. \tag{43}$$

here k_{pe} is the reaction rate constant between the anode particle to the electrolyte. The molar flux of Li from the plated Li to the anode particle, m_{pa}, is given by

$$m_{\text{pa}} = 2k_{\text{pa}} \sqrt{\frac{(c_a^{\max} - c_a|_{r_a=R_a}) c_a|_{x=R_a}}{V_{Li}}} \sinh\left(\frac{F\eta_{\text{pa}}}{2RT}\right), \tag{44}$$

where η_{pa} is the overpotential between plating to the anode particles given by

$$\eta_{\text{pa}} = U_{eq,a}(c_a|_{r_a=R_a}) - \Delta, \tag{45}$$

where k_{pa} is reaction rate constant.

The full cell Voltage For Specified galvanostatic current $I(t)$ can be used to compute the potentials at the anode and cathode current collectors V_a and V_c, respectively via the relations $V_a(t) = \Phi_a|_{x=L_0}, V_c(t) = \Phi_c|_{x=L_c}$ and hence the potential drop across the full cell (i.e. the cell voltage) is given by

$$V(t) = V_c(t) - V_a(t) - \mathcal{R}_{cont} I(t). \tag{46}$$

where $\mathcal{R}_{cont}$ is the contact resistance of the cell.

3 Analytic parameter functions

Diffusivity in anode and cathode are assumed to depend on Arrhenius temperature and are given below

$$D_{a,c}(c_{a,c}, T) = D_{a,c}(c_{a,c}) \exp\left(\frac{E_{a,c}}{R\hat{T}} - \frac{E_{a,c}}{RT}\right) \tag{47}$$

where

$$\begin{aligned} D_a(c_a) &= 0.085(9.9 \times 10^{-14} \exp\left(-59.23 c_a^2\right) + 3.053 \times 10^{-14} \exp\left(-82.6446\left(c_a - 6.6 \times 10^{-4}\right)\right)^2 \\ &\quad + 3.6840 \times 10^{-14} \exp\left(-18.1818\left(c_a - 0.6236\right)\right)^2 + 1.8420 \times 10^{-14} \exp\left(-31.25\left(c_a - 0.6236\right)\right)^2 \\ &\quad + 3.517 \times 10^{-14} \exp\left(-40\left(c_a - 0.6169\right)\right)^2 + 7.12 \times 10^{-14} \\ D_c(c_c) &= 3.7 \times 10^{-15} - 3.4 \times 10^{-15} \exp\left(-12\left(c_c - 0.62\right)^2\right) \end{aligned} \tag{48}$$

Reaction rate constants

$$k_{ae,ce} = k_{ae0,ce0} \exp\left(\frac{E^k_{a,c}}{R\hat{T}} - \frac{E^k_{a,c}}{RT}\right) \tag{49}$$

where $E^k_{a,c}$ and $E_{a,c}$ are the activation energies, $k_{ae0,ce0}$ are the reaction rate constants at the reference temperature and are given in Table 1 of the main paper, and $\hat{T}$ is the reference temperature of 22.85°C.

Open circuit potential for graphite

$$\begin{aligned} U_{eq,a}(c_a) &= 0.7165 \exp(-369.03 c_a) + 0.1219 \exp(-35.648(c_a - 0.053095)) - 0.018919 \\ &\quad \tanh(21.197(c_a - 0.19618)) - 0.016964 \tanh(27.137(c\_0.31283)) - \\ &\quad 0.019931 \tanh(28.57(c_a - 0.61422)) - 0.93115 \exp(36.328(c_a - 1.1074)) \\ &\quad + 0.01 \log(1 - c_a) + 0.14003. \end{aligned} \tag{50}$$

Open circuit potential for NMC622

$$\begin{aligned} U_{eq,c}(c_c) &= -1.28981 c_c + 0.689664 \tanh(-1.50306(c_c - 0.14723)) \\ &\quad + 0.13299 \tanh(3.71468(c_c - 0.586273)) - 7.72233 \tanh(0.225741(c_c - 2.68127)). \end{aligned} \tag{51}$$

4 Parametrisation from experimental data in Sanders et. al[2]

Proper parametrisation is crucial to maximise the predictive capability of physics-based models[3]. Furthermore, the DFN model, and to a lesser extend the SPM model, are susceptible to over-fitting due to the large number of scalar parameters and scalar functions. To avoid this we leverage data provided by the manufacturer or measurements performed directly on the cell in question wherever possible. In lieu of this we turn to the literature and take values measured by experiment on other cells. This leaves us needing to fit 6 scalar parameters: (i) reaction rates constants k_{ae}, k_{ce}, k_{pa} and $A_{pe}k_{\text{pe}}$ (we emphasize that the latter always appears as a product and therefore only counts as a single fitting parameter), (ii) the volume fraction available for Li plating in the surface film $\xi_p^\bullet$, and (iii) the area of nucleation sites ($\mathcal{N}$). The parameters used are summarised in Table 1 in main paper. The cathode was cut to 1.9 cm $\times$2.9 cm (5.51×10^{-4} m^2) whereas the anode was cut to 2.1 cm $\times$ 3.1 cm (6.51×10^{-4} m^2). Anode-to-cathode ratios in commercial cells are usually always larger than 1. The anode region which has no cathode counter-part is often called the overhang anode. Transportation of Li from/to these regions is known to cause reversible capacity effects taking place at varied timescales. We take both electrode cross-section areas to be 5.51×10^{-4}m^2 on the basis that Li transport out of the overhang is insignificant compared to Li transportation in rest of the cell. Areal capacity of graphite is 4.4 mAh cm^{-2} and mass is 14.79 mg cm^{-2}. This gives 297.5 mAh g^{-1} capacity and the theoretical capacity of graphite is 372 mAhg^{-1}, so we can use this to estimate that 80% of the anode is graphite. Then the maximum volume of Li in graphite will be approximately 32.9 mol L^{-1} (32800 mol m^{-3})[4,5]. Similarly, the maximum Li concentration in NMC622 is fitted to 42000 mol m^{-3}. Since 80% anode is graphite and 80% cathode is NMC622. The volume fraction of graphite particles in the anode and cathode is 0.9497 and 0.8235 respectively. These values are adjusted according to the dimensions of the anode and cathode. For initial concentration in both electrodes fitted with a good initial guess[4,5] and then adjusted with the voltage output to the experiment data. it has been observed that in the initial stages SEI can grow up to 100 nanometre[6–9] and we assumed that the SEI is 100 nanometres thick. Diffusivity in anode and cathode is the function of the concentration Fig. 3. We have used the diffusivity in anode from[4] and cathode from[4,10] and $U_{eq,a}$ in anode from[4] given in Fig. 3(c) and $U_{eq,c}$ was obtained by charging a half cell with an NMC622 electrode to 4.2V at a rate of C/140 in our simulation we have fitted the experimental data with the analytical function given in (51) and plotted in Fig. 3(d) of the main paper. All the fitted analytic functions are given in SI §3. Butler-Volmer reaction rate constants are fitted. In order to fit electrolyte resistance $R_e = \mathcal{L}/\kappa A\mathcal{B}$, where $\mathcal{L}$ is the distance between the representative anode and cathode particles which is provided by the manufacturer i.e. the thickness of both electrodes (50 $\mu\dot{\text{m}}$) and separator is (10 $\mu\dot{\text{m}}$ and electrode cross-section A. κ conductivity of electrolyte, $\mathcal{B}$ permeability are taken from the LiionDB database (www.liiondb.com)[3] and[4,5,11–13]. We would like to emphasises that in our experience we observe that k_{pa} is negligible compared to the other reaction rate constant and the model can predict the experiment's results for $k_{\text{pa}} = 0$ which implies $m_{\text{pa}} = 0$. This suggests that Li recovery pre-dominantly occurs via the electrolyte (rather than via direct transport between the plate and graphite)

5 Model validation with Ge *et al.*[14]

In this section, we have validated our SPM with the Li plating model (given in §2 of the main paper) with the experiments from[14]; we have managed to obtain excellent agreement having adjusted only two parameters (the reaction rate constants). We shall only discuss the validation results but refer readers to see the work of Ge *et al.*[14] for full detail. All the parameters are taken from[14] with the exception of the reaction rate constants which must be adjusted to account for the difference in how we define our BV reaction rate. Initial concentrations in the anode and cathode were fitted by comparison with the experiment data. Fig. 2, shows the plot of the discharge voltage curves for C-rate C/20 (black), 0.65C (red), 1.3C (blue), and 2.6C (magenta) at 25°C and at 5°C. Experimental data is marked by square symbols and model simulation by solid lines. Discharge curves are very similar for 0.65C and 1.3C, for both temperatures. However, at 2.6C there is a significant difference when the temperature drops from 25°C to 5°C.

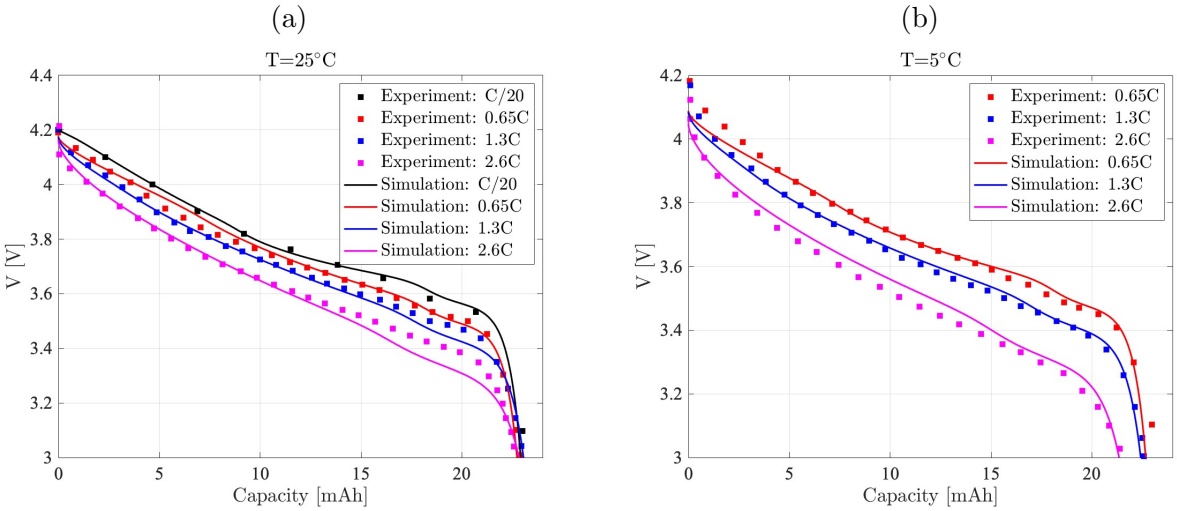

Figure 2: (a) Discharge voltage curve for C/20 (black), 0.65C (red), 1.3C (blue), and 2.6C (magenta) at 25°C. (b) discharge voltage curve for 0.65C (red), 1.3C (blue), and 2.6C (magenta) at 5°C . In both panels experiment data marked as a square symbol and model simulation results by solid lines.

References

[1] I. Korotkin, S. Sahu, S. E. J. O'Kane, G. Richardson and J. M. Foster, Journal of The Electrochemical Society, 2021, **168**, 060544.

[2] K. J. Sanders, A. R. Aguilera, J. R. Keffer, B. J. Balcom, I. C. Halalay and G. R. Goward, Carbon, 2022, **189**, 377–385.

[3] A. A. Wang, S. E. J. O'Kane, F. B. Planella, J. L. Houx, K. O'Regan, M. Zyskin, J. Edge, C. W. Monroe, S. J. Cooper, D. A. Howey, E. Kendrick and J. M. Foster, Progress in Energy, 2022, **4**, 032004.

[4] M. Ecker, T. K. D. Tran, P. Dechent, S. Käbitz, A. Warnecke and D. U. Sauer, Journal of The Electrochemical Society, 2015, **162**, A1836–A1848.

[5] M. Ecker, S. Käbitz, I. Laresgoiti and D. U. Sauer, Journal of The Electrochemical Society, 2015, **162**, A1849–A1857.

[6] W. Huang, P. M. Attia, H. Wang, S. E. Renfrew, N. Jin, S. Das, Z. Zhang, D. T. Boyle, Y. Li, M. Z. Bazant, B. D. McCloskey, W. C. Chueh and Y. Cui, Nano Letters, 2019, **19**, 5140–5148.

[7] B. Horstmann, J. Shi, R. Amine, M. Werres, X. He, H. Jia, F. Hausen, I. Cekic-Laskovic, S. Wiemers-Meyer, J. Lopez, D. Galvez-Aranda, F. Baakes, D. Bresser, C.-C. Su, Y. Xu, W. Xu, P. Jakes, R.-A. Eichel, E. Figgemeier, U. Krewer, J. M. Seminario, P. B. Balbuena, C. Wang, S. Passerini, Y. Shao-Horn, M. Winter, K. Amine, R. Kostecki and A. Latz, Energy Environ. Sci., 2021, **14**, 5289–5314.

[8] H. J. Ploehn, P. Ramadass and R. E. White, Journal of The Electrochemical Society, 2004, **151**, A456.

[9] A. Wang, S. Kadam, H. Li, S. Shi and Y. Qi, npj Computational Materials, 2018, **4**, 15.

[10] O. Chaouachi, J.-M. Réty, S. Génies, M. Chandesris and Y. Bultel, Electrochimica Acta, 2021, **366**, 137428.

[11] S. E. J. O'Kane, W. Ai, G. Madabattula, D. Alonso-Alvarez, R. Timms, V. Sulzer, J. S. Edge, B. Wu, G. J. Offer and M. Marinescu, Phys. Chem. Chem. Phys., 2022, **24**, 7909–7922.

[12] S. G. Marquis, V. Sulzer, R. Timms, C. P. Please and S. J. Chapman, Journal of The Electrochemical Society, 2019, **166**, A3693–A3706.

[13] G. Richardson, I. Korotkin, R. Ranom, M. Castle and J. Foster, Electrochimica Acta, 2020, **339**, 135862.

[14] H. Ge, T. Aoki, N. Ikeda, S. Suga, T. Isobe, Z. Li, Y. Tabuchi and J. Zhang, Journal of The Electrochemical Society, 2017, **164**, A1050–A1060.